

Conference Paper

Electrical Properties of Tungstates $\text{Ln}_2(\text{WO}_4)_3$ (Ln – Gd, Ho)

D.A. Lopatin, A.F. Guseva, N.N. Pestereva, E.L. Vostrotina, and L.I. Baldina

Institute of Natural Sciences, Ural Federal University, 620000 Ekaterinburg, Russia

Abstract

Electrical properties of $\text{Gd}_2(\text{WO}_4)_3$ and $\text{Ho}_2(\text{WO}_4)_3$ were studied and the type of charge carriers was determined. The studied compounds have a salt-like structure with isolated tetrahedrons. It crystallises in the $\text{Eu}_2(\text{WO}_4)_3$ structural type, so-called 'defective scheelite', in which 1/3 of Ln sites are vacant, $\text{Ln}_{2/3}[\text{V}_{\text{Ln}}]_{1/3}\text{WO}_4$. Predominant ionic conductivity in $\text{Ln}_2(\text{WO}_4)_3$ (Ln = Gd, Ho) was established both by the EMF method and from independence of conductivity versus oxygen partial pressure. A minor contribution (4-11%) of the anion $[\text{WO}_4]^{2-}$ transport was detected by the Tubandt method, which along with the results of the EMF technique proves the predominant oxygen conductivity.

Keywords: lanthanide tungstates, ion transference numbers, Tubandt method, electrical conductivity versus temperature, oxygen partial pressure

Corresponding Author: N.N.

Pestereva; email:

Natalie.Pestereva@urfu.ru

Received: 9 September 2016

Accepted: 19 September 2016

Published: 12 October 2016

Publishing services provided
by Knowledge E

© D.A. Lopatin et al. This article is distributed under the terms of the [Creative Commons Attribution License](#), which permits unrestricted use and redistribution provided that the original author and source are credited.

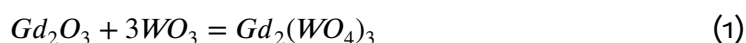
Selection and Peer-review under the responsibility of the ASRTU Conference Committee.

1. Introduction

It has been established earlier [1, 2] that electromigration in tungstates with the structure of scheelite is carried by ions O^{2-} and WO_4^{2-} . Since the polyanionic transfer is a rare and insufficiently studied phenomenon, that is of interest to investigate the type and the nature of the conductivity of trivalent metal tungstates, for example $\text{Gd}_2(\text{WO}_4)_3$ and $\text{Ho}_2(\text{WO}_4)_3$. This tungstates crystallizes in $\text{Eu}_2(\text{WO}_4)_3$ structural type, so-called 'defective scheelite', in which 1/3 of Me-sites are vacant, $\text{Me}_{2/3}[\text{V}_{\text{Me}}]_{1/3}\text{WO}_4$ [3, 4]. The crystal structure of 'defective scheelite' can be characterized by the presence of isolated tetrahedrons $[\text{WO}_4]$, which have a common oxygen apex with $[\text{MeO}_8]$ dodecahedrons [3, 4].

2. Methods

$\text{Gd}_2(\text{WO}_4)_3$ was prepared by the solid-state method from the powders of Gd_2O_3 and WO_3 of the 'extra-pure grade' qualification in air. The oxides Gd_2O_3 and WO_3 were previously calcinated for 6 hours to remove traces of moisture, Gd_2O_3 at 1100°C , WO_3 at 800°C . Synthesis was performed according to the equation:



OPEN ACCESS

with the gradual increase of temperature (600-1100°C) in six steps with intermediate grindings in the ethyl alcohol media; annealing time at each stage varied from 12 to 96 hours.

$\text{Ho}_2(\text{WO}_4)_3$ was prepared by glycerole-nitrate method described in Ref. [5]. The precursors for glycerole-nitrate method were $(\text{NH}_4)_{10}\text{W}_{12}\text{O}_{41}$, Ho_2O_3 , $\text{C}_4\text{H}_6\text{O}_6$, and 57% HNO_3 (all of high purity grade). The phase purity of the samples was confirmed by X-ray diffraction (XRD) method (Bruker D8 ADVANCE, Cu-K_α radiation, 40 kV, 40 mA, exposition 1 s, angles range $15 \leq 2\theta \leq 65$). The unit cell parameters were refined by the FullProf Package.

Compacted briquettes of $\text{Ln}_2(\text{WO}_4)_3$ with a diameter of 1 cm and 2 mm thickness were obtained by pressing of powders at 900 kg/cm² followed by sintering at 1100°C for 24 hours ($\text{Gd}_2(\text{WO}_4)_3$) and 900°C for 48 hours ($\text{Ho}_2(\text{WO}_4)_3$). The relative densities of the ceramic samples were 85% for $\text{Gd}_2(\text{WO}_4)_3$ and 60% for $\text{Ho}_2(\text{WO}_4)_3$. $\text{Ln}_2(\text{WO}_4)_3$ (Ln = Gd, Ho) samples resistance was measured by impedance spectroscopy with the Immittance Parameters Meter IPI1 (Trapeznikov Institute of Control Sciences, Moscow) at frequencies of 100 Hz - 1 MHz in the temperature range 450-880°C.

The sum of ionic transference numbers was determined by the EMF method in the cell:

$$P'_{\text{O}_2}(\text{Pt}) | \text{Ln}_2(\text{WO}_4)_3 | (\text{Pt}) P''_{\text{O}_2} \quad (2)$$

The effect of oxygen partial pressure P_{O_2} on conductivity was measured at fixed temperature in the temperature range 700-940°C. The oxygen pressure was set and controlled by an oxygen pump and a sensor made of solid electrolyte on the basis of yttrium-stabilised zirconia $\text{ZrO}_2(\text{Y}_2\text{O}_3)$.

The nature of mass and charge transfer was determined by the Tubandt method in a two-piece cell:

$$(-)\text{Pt} | \text{Ln}_2(\text{WO}_4)_3 | \text{Ln}_2(\text{WO}_4)_3 | \text{Pt}(+) \quad (3)$$

The experiment was carried out at 850°C; the voltage $U = 300$ V was applied to Cell with the current not exceeding 1 mA. The amount of electricity passing through the cell Q ranged from 10 to 86 C. The TG and DSC measurements were carried out with the simultaneous thermal analysis device NETZSCH STA 409 PC LUXX equipped with the Quadrupole Mass Spectrometer QMS 403 AËLOS.

3. Results

3.1. Phase identification

$\text{Gd}_2(\text{WO}_4)_3$ and $\text{Ho}_2(\text{WO}_4)_3$ were confirmed to be a single phase by XRD analysis (Fig. 1). The unit cell parameters of the synthesised phases are in good agreement with the published earlier (Table 1) [6].

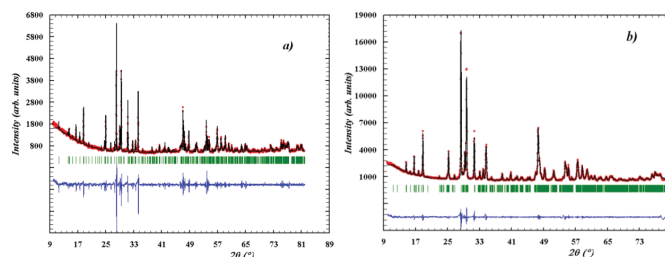


Figure 1: XRD patterns $\text{Gd}_2(\text{WO}_4)_3$ $\text{Ho}_2(\text{WO}_4)_3$.

Substance	Unit cell parameters (lit.) [6]				Unit cell parameters (exp.)			
	a	b	c	β	a	b	c	β
$\text{Gd}_2(\text{WO}_4)_3$	7,656	11,413	11,388	109,62°	7,672	11,409	11,441	109,60°
$\text{Ho}_2(\text{WO}_4)_3$	7,579	11,283	11,256	109,42°	7,581	11,819	11,263	109,42°

TABLE 1: The unit cell parameters of $\text{Ln}_2(\text{WO}_4)_3$ ($\text{Ln} = \text{Gd}, \text{Ho}$).

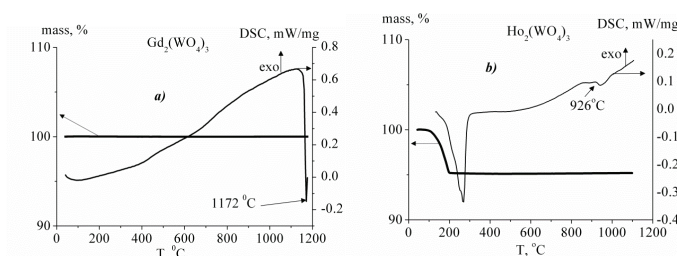


Figure 2: TGA and DSC results for $\text{Ln}_2(\text{WO}_4)_3$.

3.2. Thermogravimetric Analysis and DSC $\text{Ln}_2(\text{WO}_4)_3$ Research

TG and DSC data are presented in Fig. 2. TG analysis showed no change in the weight of the $\text{Gd}_2(\text{WO}_4)_3$ samples in the entire temperature range under study. Mass loss at 150 for tungstate holmium associated with dehydration due to its hygroscopicity. Endothermal effect at 1172°C on the DSC curve of $\text{Gd}_2(\text{WO}_4)_3$ and 926°C on the DSC curve of $\text{Ho}_2(\text{WO}_4)_3$ can be interpreted as the phase transformation from low-temperature defect scheelite $\text{Eu}_2(\text{WO}_4)_3$ structure to the high-temperature $\text{Sc}_2(\text{WO}_4)_3$ type structure [6].

3.3. Electrical Conductivity and Transference Numbers of $\text{Ln}_2(\text{WO}_4)_3$

The resistance of $\text{Ln}_2(\text{WO}_4)_3$ samples was measured by impedance spectroscopy. The temperature dependences of the conductivity of the $\text{Ln}_2(\text{WO}_4)_3$ are shown in Fig. 3. The jump in conductivity $\text{Ho}_2(\text{WO}_4)_3$ at 850°C is probably due to the phase transition, the nature of which is not yet clear.

Conductivity value of both phases is almost identical (Fig. 3) below 850°C, due to close radii values of Ln^{3+} (Gd^{3+} - 0.1193 nm, Ho^{3+} - 0.1155 nm) [7] and due to the same phase structure. But above 850°C $\text{Ho}_2(\text{WO}_4)_3$ conductivity is 7-8 times higher than for

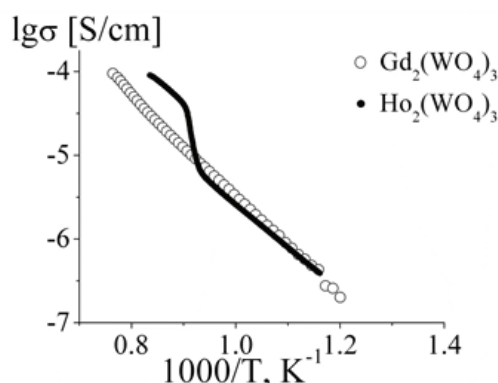


Figure 3: Temperature dependence of conductivity for $\text{Ln}_2(\text{WO}_4)_3$.

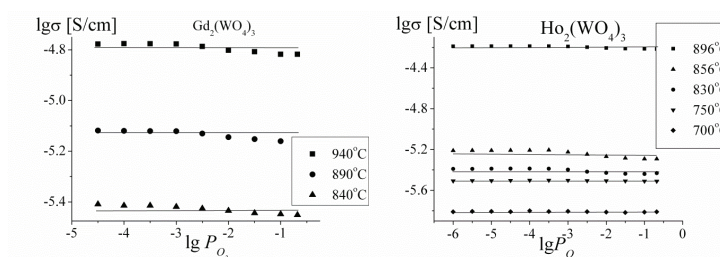


Figure 4: Oxygen pressure dependence of conductivity for $\text{Ln}_2(\text{WO}_4)_3$.

$\text{Gd}_2(\text{WO}_4)_3$. This fact can probably be explained by the $\text{Ho}_2(\text{WO}_4)_3$ phase transition at 850°C .

The conductivity isotherms of $\text{Ln}_2(\text{WO}_4)_3$ versus oxygen partial pressure are shown in Fig. 4. The fact of independence of the value of total conductivity with oxygen pressure may confirm the ionic conductivity in $\text{Ho}_2(\text{WO}_4)_3$ and $\text{Gd}_2(\text{WO}_4)_3$ within the temperature range $700\text{--}940^\circ\text{C}$. $\sum t_{ion}$ of $\text{Gd}_2(\text{WO}_4)_3$ measured by EMF method is close to 1. This fact is in a good agreement with the independence of the $\text{Gd}_2(\text{WO}_4)_3$ electrical conductivity of the P_{O_2} (Fig. 4).

3.4. The Nature of Mobile Carriers in $\text{Ln}_2(\text{WO}_4)_3$ (Tubandt method)

To clarify the type of charge carriers for $\text{Ln}_2(\text{WO}_4)_3$, Tubandt experiments were carried out in a two-section cell at 850°C . Mass loss of the cathode section and growth of the anode section weight were found (Fig. 5).

Reproducible mass reduction of the cathode section proved that negative ions were responsible for the charge transfer. Since the transfer of oxygen ions cannot lead to a change in mass of the samples, the experimentally observed change in mass of cathode and anode sections are due to the $[\text{WO}_4]^{2-}$ transfer. If this supposition is correct, then a phase enriched by lanthanide and a phase enriched by tungsten should appear in the cathode space and in the anode space, respectively. The XRD results of the cathode and anode areas of $\text{Ho}_2(\text{WO}_4)_3$ briquettes are shown in Fig. 6. Indeed, XRD

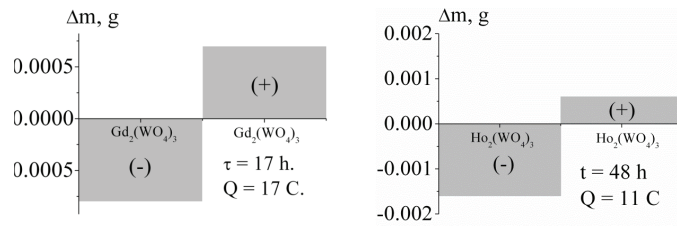


Figure 5: Diagrams of mass variations for ceramic $Gd_2(WO_4)_3$ and $Ho_2(WO_4)_3$, $T = 850^\circ C$.

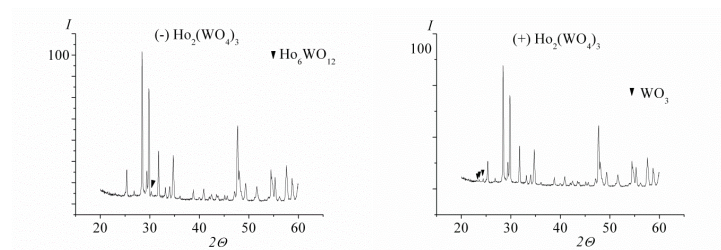
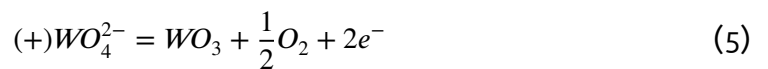
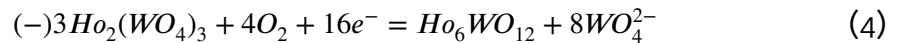


Figure 6: XRD patterns of the cathode (a) and anode (b) areas of briquettes $Ho_2(WO_4)_3$.

pattern of the $Ho_2(WO_4)_3$ cathode briquette surface with was in contact with the Pt(-) electrode reveals an appearance of a phase enriched by holmium (Ho_6WO_{12}). At the same time, a phase enriched by tungsten (WO_3) was identified on the surface of the anode briquette $Ho_2(WO_4)_3$ in contact with the Pt(+) electrode.

Possible electrode reactions that can occur in the cathode and anode sections are:



By using the Faraday's law and assuming that the amount of mass loss of the cathode section $\Delta m^{(-)}$ is correspondent to the WO_3 mass related to the migration of $[WO_4]^{2-}$ ions, the $[WO_4]^{2-}$ ion transference number was calculated according to the formula:

$$t_{WO_4^{2-}} = \frac{\Delta m^{(-)}}{M_{WO_3}} \cdot z_{WO_4^{2-}} \cdot \frac{F}{Q}, \quad (6)$$

where WO_3 is WO_3 molar mass (g/mol), $z = 2$, Q is the amount of electricity passed through the system (C), F is Faraday's constant.

The molar mass of WO_3 M_{WO_3} (instead of $M_{WO_4^{2-}}$) was used in the formula, because according to the equation of reaction (4), the mass loss of the cathode section caused by the disappearing of tungsten oxide is the following:

$$\Delta m^{(-)} = m(WO_4^{2-}) - m(\frac{1}{2}O_2) \quad (7)$$

The transference numbers of tungstate ion calculated according to the Eq. (6) are about 4% for gadolinium tungstate and 11% for holmium tungstate.

The obtained results indicate that $[\text{WO}_4]^{2-}$ makes no significant contribution to the charge transfer in the studied systems; therefore, the particles that do not affect the mass change play a predominant role. Thus, one can conclude that oxygen ions can serve as mobile species, i.e., $t(\text{O}^{2-}) \gg t(\text{WO}_4^{2-})$.

This result is quite unexpected, because contribution of tungstate ion in the electric transport for isostructural divalent metal tungstates (CaWO_4 , SrWO_4 , BaWO_4) according to the data [2], is much higher, and varies from 20 to 50%. The insignificant contribution of $[\text{WO}_4]^{2-}$ transfer to the electrotransport of $\text{Ho}_2(\text{WO}_4)_3$ and $\text{Gd}_2(\text{WO}_4)_3$ with the defect scheelite structure (as compared with the divalent metal tungstates) can be due to the fact that structural vacancies V_{Ln} open channels for the O^{2-} migration that increase the contribution of oxygen conductivity.

4. Conclusion

Thus, the set of the experimental results suggests that O^{2-} ions are the main charge carriers in the tungstates $\text{Ln}_2(\text{WO}_4)_3$ ($\text{Ln} = \text{Ho}, \text{Gd}$). Together with that, a minor (under 11%) contribution of polyanions $[\text{WO}_4]^{2-}$ into the ion transport was detected.

Acknowledgement

The research results were obtained in the framework of the State Task of the Ministry of Education and Science of Russia and supported by the grants of the Russian Foundation for Basic Research RFBR 14-03-00804_a. The equipment of the Ural Center for Shared Use "Modern nanotechnology" UrFU was used.

References

- [1] Y. Zhou, S. Adams, R. P. Rao, D. D. Edwards, A. Neiman, and N. Pestereva, Charge transport by polyatomic anion diffusion in $\text{Sc}_2(\text{WO}_4)_3$, *Chemistry of Materials*, **20**, no. 20, 6335–6345, (2008).
- [2] A. Y. Neiman, N. N. Pestereva, Y. Zhou, D. O. Nechaev, E. A. Koteneva, K. Vanec, B. Higgins, N. A. Volkova, and I. G. Korchuganova, The nature and the mechanism of ion transfer in tungstates Me_2WO_4 ($\text{Ca}, \text{Sr}, \text{Ba}$) and Me_2WO_3 ($\text{Al}, \text{Sc}, \text{In}$) according to the data acquired by the tubandt method, *Russian Journal of Electrochemistry*, **49**, no. 9, 895–907, (2013).
- [3] A. A. Evdokimov and V. A. Efremov, *Trunov VK: Compounds of rare earth elements. Molybdates, tungstates*. Moscow, Nauka, Moscow, 1991.
- [4] M. A. Poraj-Koshice, *Atovmyan LO: Crystal chemistry and stereochemistry of coordination compounds of molybdenum*, Nauka, Moscow, 1974.
- [5] N. N. Pestereva, I. G. Safonova, S. S. Nokhrin, and A. Y. Neiman, Effect of MWO_4 ($\text{M} = \text{Ca}, \text{Sr}, \text{Ba}$) dispersion on the interfacial processes in $(+/-)\text{WO}_3|\text{MWO}_4|\text{WO}_3(-/+)$ cells and transport properties of metacomposite phases, *Russian Journal of Inorganic Chemistry*, **55**, no. 6, 876–882, (2010).
- [6] L. F. Grigorieva, *Diagrams of refractory oxide systems*, Nauka, Leningrad, 1988.
- [7] R. D. Shannon and A. Acta Crystallogr. Sect., (1976), 751.